[PROC. OF JSCE No. 412/III-12 (Geotechnical Eng.) December 1989]

A NUMERICAL EVALUATION METHOD OF WAVES IN ROCK MASS WITH CRACKS

By *Sixiong HAN*, Yasuaki ICHIKAWA** and Toshikazu KAWAMOTO****

The problem of elastic wave travelling in rock mass that usually contains cracks, involves several difficulties from the theoretical point of view. In this paper, a new model to treat such problems is proposed, in which, instead of modelling the cracks directly, the mechanical effects of cracks are transformed into an equivalent nodal force in a numerical procedure. Accordingly, the response is obtained by the superposition of the incident wave field and the scattering wave field which is produced by the radiation of the reflected waves from the crack surfaces. Finally, a numerical example is given and it is shown that the calculated results by the proposed method is in very good agreement with those of the exact ones.

Keywords : *elastic wave, cracks, displacement gap, equivalent nodal force, finite element method*

1. INTRODUCTION

Internal cracks distributed in rock mass give much influence for elastic wave propagation. When a large rock structure such as the underground power house and the dam is planed to construct, the problem of wave propagation is much considered in terms of aseismatic design. However, this problem has not been solved satisfactorily yet. One of the main reason is that the geological discontinuities such as cracks and faults make this problem become complex.

Several approaches have been proposed in order to treat this problem, which can be categorized into two groups : The first is to obtain analytical solutions in the form of integral equation[8),11),13)]. Another is based on the approximate and empirical method. One may introduce some simple models which account for the reflection and transmission characteristics of waves at the crack surface[1)]. The kinematical condition is usually disregarded. Then, the model parameters are determined by experiences or some simple experiments.

This paper deals with the problem of wave propagation in rock mass which contains individual cracks. The behaviour of each crack is modelled in the form of displacement gap, then its effect is evaluated as an equivalent body force[4)]. We propose a numerical method involving the above body force term.

2. MODELING OF WAVE PROPAGATION IN MATERIAL WITH DISCONTINUITIES

In a homogeneous isotropic linear elastic body D, we consider two kinematic states with displacements u_i and v_i, and with body forces H_i and E_i.

* M. Eng., Doctorate Student, Department of Geotechnical Engineering, Nagoya University (Chikusa, Nagoya 464)
** Member of JSCE, Dr. Eng., Associate Professor, Department of Geotechnical Engineering, Nagoya University (ditto)
*** Member of JSCE, Dr. Eng., Professor, Department of Geotechnical Engineering, Nagoya University (ditto)

The Betti's reciprocal principle states that

$$\int_D \left\{\left(\frac{\partial^2 u_i}{\partial t^2}-H_i\right)v_i-\left(\frac{\partial^2 v_i}{\partial t^2}-E_i\right)u_i\right\}\rho dv$$
$$=\int_B (t_i^u v_i - t_i^v u_i)ds \cdots\cdots (1)$$

where t_i^u and t_i^v are the tractions with respect to u_i and v_i respectively, and ρ is the mass density. Note that the boundary B of the body D consists of the displacement one B_u and the force one B_t.

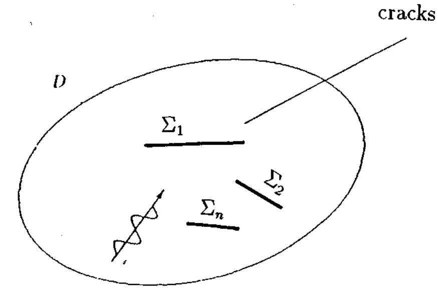

Fig. 1 Discontinuous material.

Let us define the convolution integral by

$$\boldsymbol{f}(x,t)*\boldsymbol{g}(x,t)=\int_0^t \boldsymbol{f}(x,\eta)\cdot \boldsymbol{g}(x,t-\eta)d\eta \cdots\cdots (2)$$

Then, the Betti's theorem can be rewritten as

$$\int_D \{(\ddot{\boldsymbol{u}}-\boldsymbol{H})*\boldsymbol{v}-(\ddot{\boldsymbol{v}}-\boldsymbol{E})*\boldsymbol{u}\}\rho dv=\int_B (\boldsymbol{t}^u * \boldsymbol{v}-\boldsymbol{t}^v * \boldsymbol{u})ds \cdots\cdots (3)$$

Taking one of the kinematic states to be induced by a unit body force impulsively applied to a particular particle at $x=\xi$ and time t in the direction of x_m-axis yields

$$\rho E_i=\delta_{im}\,\delta(t)\,\delta(x-\xi) \cdots\cdots (4)$$

where the three-dimensional Dirac delta function $\delta(x-\xi)$ and one-dimensional Dirac delta function $\delta(t)$ indicate the spatial location and the timing of the impulse, respectively, and the Kronecker delta function δ_{im} specifies the directional property. The displacement response function given by $v_i=G_i^m(x,\xi,t)$ is the i-th component of displacement at the point x due to a unit point force acting at ξ in the direction of x_m-axis with time variation $\delta(t)$ ($G_i^m(x,\xi,t)$ is the Green's function). Thus, the response in displacement field can be obtained as

$$u_m(\xi,t)=\int_D \rho H_i(x,t)*G_m^i(\xi,x,t)dv+\int_{Bt} t_i^u * G_m^i(\xi,x,t)ds-\int_{Bu} u_i(x,t)*C_{ijpq}n_j\frac{\partial G_m^q}{\partial x_p}ds \cdots\cdots (5)$$

where $\boldsymbol{n}$ represents the unit vector normal to the boundary B and C the Hooke's tensor. For an isotropic linear elastic body, it has the form

$$C_{ijkl}=\lambda\delta_{ij}\delta_{kl}+\mu(\delta_{ik}\delta_{jl}+\delta_{il}\delta_{jk}) \cdots\cdots (6)$$

It involves only two independent constants, λ and μ, known as the Lame's constants.

The second and third terms of the right hand side of Eq. (5) describe the scattering effects of waves on the boundaries B_u and B_t, respectively.

Let us consider cracks $\sum_k (k=1, \cdots\cdots, n)$ in the body D (Fig. 1). Note that on $\sum_k$ the stress and displacement are discontinuous. Each crack $\sum_k$ is regarded as an interior boundary, and we assume that the boundaries except for $\sum_k$ satisfy a stress free condition. Therefore, from the relation (5) the response induced by the scattering waves on the cracks is obtained as

$$u_m^s=-\sum_{k=1}^{n}\int_{\Sigma k}\left\{\Delta t_i^u(u,x,t)*G_m^i(\xi,x,t)-C_{ijpq}n_j\,\Delta u_i(x,t)*\frac{\partial G_m^p(\xi,x,t)}{\partial x_q}\right\}ds \cdots\cdots (7)$$

where the symbol "$\Delta(\cdot)$" represents the gap of "$\cdot$" across the discontinuous surface $\sum_k$. That is, $\Delta(\cdot)=(\cdot)|_{\Sigma^+_k}-(\cdot)|_{\Sigma^-_k}$ where $\sum_k^+$ and $\sum_k^-$ are both sides of the $\sum_k$. By using the Delta function $\delta(x-\xi)$ in the above formula, it can be shown that the effect of cracks is accounted by the following form of an equivalent body force:

$$F_i(x,t)=-\sum_{k=1}^{n}\int_{\Sigma k}\left(\Delta t_i^k(u,\xi,t)\,\delta(x-\xi)-C_{pjiq}n_j^k\frac{\partial\delta(x-\xi)}{\partial x_q}\Delta u_p^k\right)ds \cdots\cdots (8)$$

where $\boldsymbol{n}^k$ is the unit vector normal of the k-th crack $\sum_k$.

Evidently, if the Green's function $G_m^i(\xi,x,t)$ in Eq. (7) is determined, the closed form solution can be obtained. It is, however, almost impossible to get the Green's function explicitly except for some specific and simple cases. Therefore, instead of obtaining the closed form solution, we will propose an alternative to evaluate the effect of cracks in terms of an equivalent body force by virtue of Eq. (8) in the following section.

3. EQUIVALENT BODY FORCE DUE TO CRACKS

We here determine the equivalent body force F_i for the plane wave condition. While the distribution and geometry of cracks in rock mass are very complicated, we simply assume that

- the cracks are all planar with no thickness,
- the cracks do not change the configuration, and
- the frequency of waves is high enough (or the wavelength is small enough with respect to the dimension of cracks), so that the Snell's Law[7] is held true on the surfaces of cracks.

The equivalent body force F_i defined by Eq. (8) consists of two parts : one is F_i^t which is induced by the traction gap, and another is F_i^u caused by the displacement gap. Thus, we have

$$\left.\begin{aligned} &F_i(x,t)=F_i^t(x,t)+F_i^u(x,t);\\ &F_i^u(x,t)=\sum_{k=1}^{n}\int_{\Sigma k} C_{pjiq}n_j^k\frac{\partial\delta(x-\xi)}{\partial x_q}\triangle u_p^k ds;\\ &F_i^t(x,t)=-\sum_{k=1}^{n}\int_{\Sigma k}\triangle t_i^k(u,\xi,t)\,\delta(x-\xi)ds; \end{aligned}\right\}\quad\cdots\cdots(9)$$

We next consider the case that cracks are open and their surfaces are stress-free, which implies that $F_i^t=0$, then we have

$$F_i(x,t)=F_i^u(x,t)=\sum_{k=1}^{n}\int_{\Sigma k}\rho f_i^k(x,\xi,t)ds\quad\cdots\cdots(10)$$

$$f_i^k(x,\xi,t)=C_{pjiq}n_j^k\frac{\partial\delta(x-\xi)}{\rho\partial x_q}\triangle u_p^k(\xi,t)\quad\cdots\cdots(11)$$

It will be shown in the followings how to determine the function $f_i^k(x,\xi,t)$ which is called the body force function.

(1) Determination of the body force function

Let us assume that the cracks are distributed in x_1x_2-plane as shown in **Fig. 2**. The unit normal to the k-th crack has the components

$\boldsymbol{n}^k=(\cos\theta^k,\ \sin\theta^k)$

The displacement gap is written as

$\triangle\boldsymbol{u}^k(\xi,t)=(u_1^{kI},u_2^{kI})$

From the relation (11), the body force function is obtained as

$$\boldsymbol{f}^k=\boldsymbol{V}^k\boldsymbol{d}^T\quad\cdots\cdots(12)$$

in which

$$\boldsymbol{V}^k=\begin{bmatrix} V_p^2u_1^{kI}\cos\theta^k+(V_p^2-2V_s^2)u_2^{kI}\sin\theta^k & V_s^2u_1^{kI}\sin\theta^k+V_s^2u_2^{kI}\cos\theta^k\\ V_s^2u_2^{kI}\cos\theta^k+V_s^2u_1^{kI}\sin\theta^k & (V_p^2-2V_s^2)u_1^{kI}\cos\theta^k+V_p^2u_2^{kI}\sin\theta^k \end{bmatrix}$$

$$\boldsymbol{d}^T=\begin{Bmatrix}\dfrac{\partial\delta(x-\xi)}{\partial x_1}\\ \dfrac{\partial\delta(x-\xi)}{\partial x_2}\end{Bmatrix}$$

where V_p and V_s denote the velocities of longitudinal and transverse waves, respectively, that is, $V_p=\sqrt{(\lambda+2\mu)/\rho}$; $V_s=\sqrt{\mu/\rho}$.

In the above representation $\boldsymbol{f}^k(x,\xi,t)$, the only unknown quantity is the displacement gap $\triangle\boldsymbol{u}^k$.

(2) Displacement gap acrossing cracks

To determine the displacement gap, let us consider time-harmonic waves. In an isotropic elastic material, the traces of the plane waves are straight lines, which are normal to the wavefront (or to the equivalent phase surface). Let an incident harmonic plane wave which has an amplitude u_0, wave number k_0 and the angular frequency ω_0 strike on the k-th crack (see Fig. 2). At the point $\boldsymbol{x}$, it has the wave form $\boldsymbol{u} = \boldsymbol{u}_0 \exp\{i(\boldsymbol{k}_0 \cdot \boldsymbol{x} + \omega_0 t)\}$ where the wave is propagating along the direction $\boldsymbol{e} = (-\cos\theta_0, -\sin\theta_0)$, $\boldsymbol{u}_0 = u_0 \boldsymbol{e}$ and $\boldsymbol{k}_0$ is wave number vector. The wavelength is so short compared with the dimension of cracks that the Snell's Law is held true on the cracks.

Let us introduce a local coordinate system $O_k\zeta$ on each crack surface. The center O_k of the k-th crack is $\boldsymbol{x}_0^k$. Then the point on the k-th crack surface is represented as $\boldsymbol{\xi} = \boldsymbol{x}_0^k + \boldsymbol{\tau}^k \zeta$ where $-\frac{l^k}{2} \leqq \zeta \leqq \frac{l^k}{2}$ (l^k is the length of the k-th crack and $\boldsymbol{\tau}^k$ the unit vector lying on it, that is, $\boldsymbol{\tau}^k = (\sin\theta^k, -\cos\theta^k)$, see Fig. 2).

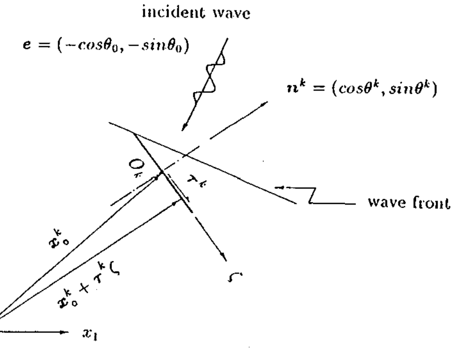

Fig. 2 Local coordinate on k-th crack.

By using these notations, Eq. (10) can be rewritten as

$$F_i(\boldsymbol{x}, t) = \sum_{k=1}^{n} \int_{-l^k/2}^{l^k/2} \rho f_i^k(\boldsymbol{x}, \boldsymbol{x}_0^k + \boldsymbol{\tau}^k \zeta, t) d\zeta. \qquad \cdots\cdots (13)$$

The following boundary conditions must be satisfied on the cracks surface :

$$\left.\begin{array}{l} (\sigma_{11}(\boldsymbol{x}, t)\cos\theta^k + \sigma_{12}(\boldsymbol{x}, t)\sin\theta^k)|_{\Sigma_k^\pm} = 0 \\ (\sigma_{21}(\boldsymbol{x}, t)\cos\theta^k + \sigma_{22}(\boldsymbol{x}, t)\sin\theta^k)|_{\Sigma_k^\pm} = 0 \end{array}\right. \quad (k = 1, \cdots\cdots, n). \qquad \cdots\cdots (14)$$

The displacement gap acrossing the crack is then obtained as

$$\begin{Bmatrix} u_n^{kI} \\ u_\tau^{kI} \end{Bmatrix} = \begin{Bmatrix} \phi_n^k(\theta^k, \zeta) \exp(i\omega_0 t) \\ \phi_\tau^k(\theta^k, \zeta) \exp(i\omega_0 t) \end{Bmatrix} \qquad \cdots\cdots (15)$$

where u_n^{kI} and u_τ^{kI} are the normal and tangential components of the displacement gap on $\sum_k$, respectively.

For an incident longitudinal wave (P-wave; Fig. 3), the parameters ϕ_n^k and ϕ_τ^k have the form

$$\begin{Bmatrix} \phi_n^k \\ \phi_\tau^k \end{Bmatrix} = \begin{Bmatrix} -u_0 \exp(i\boldsymbol{k}_o \cdot \boldsymbol{x}_o^k + i\boldsymbol{k}_o \cdot \boldsymbol{\tau}^k \zeta)\cos(\theta_0 - \theta^k) + u_p^k \exp(i\boldsymbol{k}_p \cdot \boldsymbol{x}_o^k + i\boldsymbol{k}_p \cdot \boldsymbol{\tau}^k \zeta)\cos(\theta_0 - \theta^k) \\ + u_s^k \exp(i\boldsymbol{k}_s \cdot \boldsymbol{x}_o^k + i\boldsymbol{k}_s \cdot \boldsymbol{\tau}^k \zeta)\sin\theta_s^k \\ u_0 \exp(i\boldsymbol{k}_o \cdot \boldsymbol{x}_o^k + i\boldsymbol{k}_o \cdot \boldsymbol{\tau}^k \zeta)\sin(\theta_0 - \theta^k) + u_p^k \exp(i\boldsymbol{k}_p \cdot \boldsymbol{x}_o^k + i\boldsymbol{k}_p \cdot \boldsymbol{\tau}^k \zeta)\sin(\theta_0 - \theta^k) \\ - u_s^k \exp(i\boldsymbol{k}_s \cdot \boldsymbol{x}_o^k + i\boldsymbol{k}_s \cdot \boldsymbol{\tau}^k \zeta)\cos\theta_s^k \end{Bmatrix}$$

and consist of the incident and reflected terms. Here u_p^k and u_s^k represent the amplitudes of reflected longitudinal and transverse waves, respectively, and k_p and k_s are the wave numbers. Note that the wave number vectors are written as $\boldsymbol{k}_0 = (-k_0\cos\theta_0, -k_0\sin\theta_0)$; $\boldsymbol{k}_p = (k_0\cos(\theta_0 - 2\theta^k), k_0\sin(\theta_0 - 2\theta^k)$; $\boldsymbol{k}_s = (k_s\cos(\theta^k - \theta_s^k), k_s\sin(\theta^k - \theta_s^k))$, in which θ_s^k is the angle between the reflected transverse wave and the normal to the k-th crack.

Using the conditions (14), the reflected wave amplitude is determined as

$$\begin{Bmatrix} u_p^k \\ u_s^k \end{Bmatrix} = \begin{Bmatrix} \dfrac{[1 - 2\lambda^2 \sin^2(\theta_0 - \theta^k)]^2 - 4\lambda^3 \sin^2(\theta_0 - \theta^k)\cos(\theta_0 - \theta^k)\sqrt{1 - \lambda^2 \sin^2(\theta_0 - \theta^k)}}{[1 - 2\lambda^2 \sin^2(\theta_0 - \theta^k)]^2 + 4\lambda^3 \sin^2(\theta_0 - \theta^k)\cos(\theta_0 - \theta^k)\sqrt{1 - \lambda^2 \sin^2(\theta_0 - \theta^k)}} u_0 \\ \dfrac{2\lambda \sin 2(\theta_0 - \theta^k)[1 - \lambda^2 \sin^2(\theta_0 - \theta^k)]}{[1 - 2\lambda^2 \sin^2(\theta_0 - \theta^k)]^2 + 4\lambda^3 \sin^2(\theta_0 - \theta^k)\cos(\theta_0 - \theta^k)\sqrt{1 - \lambda^2 \sin^2(\theta_0 - \theta^k)}} u_0 \end{Bmatrix}$$

$$k_0 = \frac{\omega_0}{V_p}; \quad k_s = \frac{\omega_0}{V_s}; \quad \lambda = \frac{k_0}{k_s}$$

Similarly, for the case of the incident transverse wave (or SV-wave; Fig. 4), we have

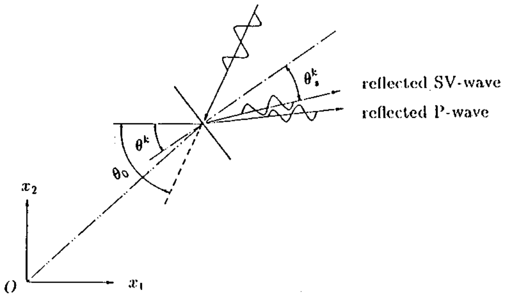

Fig. 3 Reflection of longitudinal plane waves.

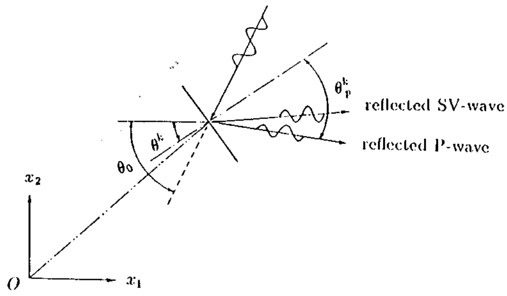

Fig. 4 Reflection of transverse plane waves.

$$\begin{Bmatrix} \phi_n^k \\ \phi_\tau^k \end{Bmatrix} = \begin{Bmatrix} u_0 \exp(i\boldsymbol{k}_o\cdot \boldsymbol{x}_o^k + i\boldsymbol{k}_o\cdot \boldsymbol{\tau}^k\zeta)\sin(\theta_0-\theta^k) + u_s^k \exp(i\boldsymbol{k}_s\cdot \boldsymbol{x}_o^k + i\boldsymbol{k}_s\cdot \boldsymbol{\tau}^k\zeta)\sin(\theta_0-\theta^k) \\ + u_p^k \exp(i\boldsymbol{k}_p\cdot \boldsymbol{x}_o^k + i\boldsymbol{k}_p\cdot \boldsymbol{\tau}^k\zeta)\cos\theta_p^k \\ u_0 \exp(i\boldsymbol{k}_o\cdot \boldsymbol{x}_o^k + i\boldsymbol{k}_o\cdot \boldsymbol{\tau}^k\zeta)\cos(\theta_0-\theta^k) - u_s^k \exp(i\boldsymbol{k}_s\cdot \boldsymbol{x}_o^k + i\boldsymbol{k}_s\cdot \boldsymbol{\tau}^k\zeta)\cos(\theta_0-\theta^k) \\ + u_p^k \exp(i\boldsymbol{k}_p\cdot \boldsymbol{x}_o^k + i\boldsymbol{k}_p\cdot \boldsymbol{\tau}^k\zeta)\sin\theta_p^k \end{Bmatrix}$$

and the reflected terms are

$$\begin{Bmatrix} u_p^k \\ u_s^k \end{Bmatrix} = \begin{Bmatrix} -\dfrac{\lambda \sin 4(\theta_0-\theta^k)}{\cos^2 2(\theta_0-\theta^k) + 4\lambda^2 \sin^2(\theta_0-\theta^k)\cos(\theta_0-\theta^k)\sqrt{\lambda^2-\sin^2(\theta_0-\theta^k)}}\, u_0 \\ -\dfrac{\cos^2 2(\theta_0-\theta^k) - 4\lambda^2 \sin^2(\theta_0-\theta^k)\cos(\theta_0-\theta^k)\sqrt{\lambda^2-\sin^2(\theta_0-\theta^k)}}{\cos^2 2(\theta_0-\theta^k) + 4\lambda^2 \sin^2(\theta_0-\theta^k)\cos(\theta_0-\theta^k)\sqrt{\lambda^2-\sin^2(\theta_0-\theta^k)}}\, u_0 \end{Bmatrix}$$

$$k_0 = \frac{\omega_0}{V_s};\quad k_p = \frac{\omega_0}{V_p};\quad \lambda = \frac{k_p}{k_0}$$

Here, the wave number vectors are obtained by $\boldsymbol{k}_0 = (-k_0\cos\theta_0,\ -k_0\sin\theta_0)$; $\boldsymbol{k}_p = (k_p\cos(\theta^k-\theta_p^k),\ k_p\sin(\theta^k-\theta_p^k))$; $\boldsymbol{k}_s = (k_0\cos(\theta_0-2\theta^k),\ k_0\sin(\theta_0-2\theta^k))$, in which θ_p^k is the angle between the reflected longitudinal wave and the normal to the k-th crack.

By the coordinate transformation, we obtained the displacement gap as

$$\begin{Bmatrix} u_1^{kl} \\ u_2^{kl} \end{Bmatrix} = \begin{bmatrix} \cos\theta^k & -\sin\theta^k \\ \sin\theta^k & \cos\theta^k \end{bmatrix} \begin{Bmatrix} u_n^{kl} \\ u_\tau^{kl} \end{Bmatrix} \quad\cdots\cdots (16)$$

One can finally calculate the equivalent body force function by substituting Eq. (15) into Eq. (16). Note that here we have considered only the harmonic waves. However by the virtue of the linear superposition principle, this method can be extended for the general incident waves.

4. FINITE ELEMENT ANALYSIS

(1) Discretization procedure

The equivalent body force obtained by Eq. (12) involves singularities, so that we cannot calculate it directly. We develop a numerical discretization scheme to avoid such singularities.

The equation of motion is discretized by introducing a finite element approximation $\{\boldsymbol{u}\} = [N]\{U\}$ and $\{\varepsilon\} = [\boldsymbol{B}]\{U\}$ where $[N]$ is the matrix of global shape functions, $[\boldsymbol{B}]$ the strain-displacement matrix, $\{U\}$ the nodal displacement vector, and $\{\varepsilon\}$ is the strain vector. One gets

$$[\boldsymbol{M}]\{\ddot{U}\} + [\boldsymbol{K}]\{U\} = \{\boldsymbol{P}\} + \{\boldsymbol{P}^*\} \quad\cdots\cdots (17)$$

Here the matrices and vectors have the forms

$$[\boldsymbol{M}] = \int_D \rho [N]^T [N] dv$$

$$[\boldsymbol{K}] = \int_D [\boldsymbol{B}]^T [\boldsymbol{D}][\boldsymbol{B}] dv$$

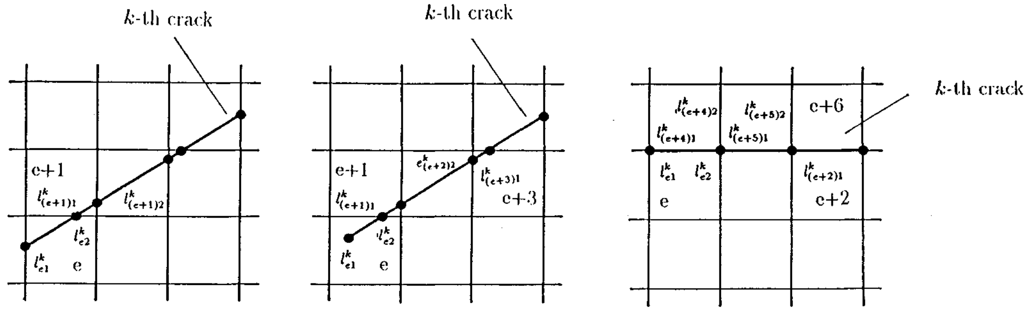

(a) a crack is crossing elements (b) a crack is included in elements (c) a crack is laid along the boundary of elements

Fig. 5 Three patterns of a crack configuration with respect to finite element.

$$\{\boldsymbol{P}\}=\left(\int_D\rho[N]^T\{\boldsymbol{H}\}dv+\int_{B_t}[N]^T\{\boldsymbol{t}\}ds\right)$$

where $\{\boldsymbol{t}\}$ is the external force vector acting on the boundary B_t, $\{\boldsymbol{H}\}$ is the body force vector introduced in Eq. (1) and $\{\boldsymbol{P}^*\}$ represents the equivalent nodal force vector induced by the cracks:

$$\{\boldsymbol{P}^*\}=\int_D[N]^T\{\boldsymbol{F}\}dv \quad\cdots\cdots (18)$$

The vector $\{\boldsymbol{F}\}$ is determined by Eq. (10).

It is then natural to ask a question how we can build in the cracks for the finite element mesh, and calculate the equivalent nodal force vector. Generally speaking, the configuration of a crack for the finite elements is classified into three kinds (Fig. 5). For each case, we calculate the equivalent nodal force vector as follows:

(Case 1)

If the tips of a crack are on the boundaries of element as shown in the Fig. 5 (a), the nodal force vector can be determined by substituting Eq. (12) and Eq. (10) into Eq. (18) as

$$\{P_i^*\}=\sum_{k=1}^{n}\int_D\int_{\Sigma_k}\rho N_{ji}V_{jk}d_k\,ds\,dv=\sum_{k=1}^{n}\int_{l^k_{e1}}^{l^k_{e2}}\rho\frac{\partial[N_{ji}]}{\partial\{\xi_q\}}\bigg|_{\xi=x^k_0+\tau^k\zeta}[V^k_{jq}]d\zeta \quad\cdots\cdots (19)$$

where l^k_{e1} and l^k_{e2} (see Fig. 5(a)) are the positions of the two points of intersection between the k-th crack and the boundary of the e-th element, respectively, in the local coordinates, and we have $\sum(l^k_{e2}-l^k_{e1})=l^k$.

(Case 2)

If a tip of a crack is within the element as shown in the Fig. 5(b), the nodal force vector has the same form as that in the case 1.

(Case 3)

When a crack is laid on the boundary of elements (Fig. 5(c)), we can use the principle of superposition to determine the nodal force vector.

Let us write a contribution of the k-th crack to the nodal force as $\{P_i^{*k}\}$. In this case, the total magnitude of the displacement gap on the k-th surface consists of the half value from each side of elements. For example shown in Fig. 5(c), we have

$$\{P_i^{*k}\}=\frac{1}{2}\left(\int_{l^k_{e1}}^{l^k_{e2}}+\int_{l^k_{(e+1)1}}^{l^k_{(e+1)2}}+\int_{l^k_{(e+2)1}}^{l^k_{(e+2)2}}\right)\rho\frac{\partial[N_{ji}]}{\partial\{\xi_q\}}\bigg|_{\xi=x^k_0+\tau^k\zeta}[V^k_{jq}]d\zeta$$
$$+\frac{1}{2}\left(\int_{l^k_{(e+4)1}}^{l^k_{(e+4)2}}+\int_{l^k_{(e+5)1}}^{l^k_{(e+5)2}}+\int_{l^k_{(e+6)1}}^{l^k_{(e+6)2}}\right)\rho\frac{\partial[N_{ji}]}{\partial\{\xi_q\}}\bigg|_{\xi=x^k_0+\tau^k\zeta}[V^k_{jq}]d\zeta \quad\cdots\cdots (20)$$

Note that, the singularity of the equivalent nodal force is eliminated in the above equations.

(2) Properties of the equivalent nodal force

In order to investigate the properties of the equivalent nodal force, let us consider a simple case of a

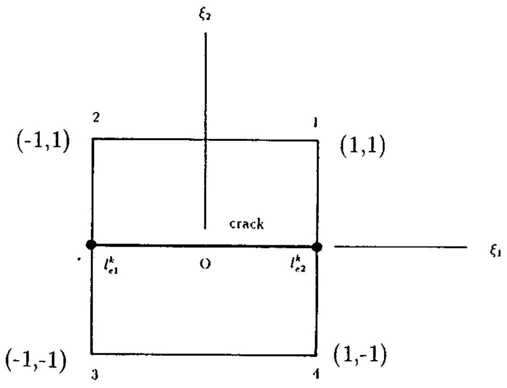

Fig. 6 Distributing state of crack in the e-th element.

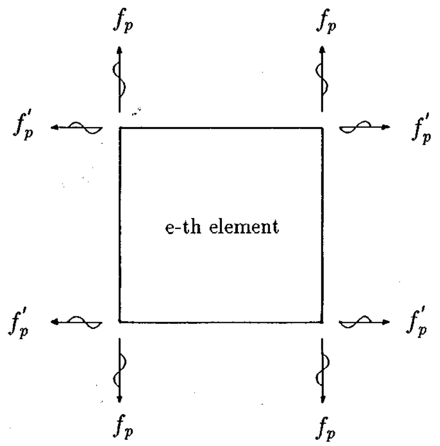

Fig. 7 (a) Equivalent nodal forces for reflected P-waves.

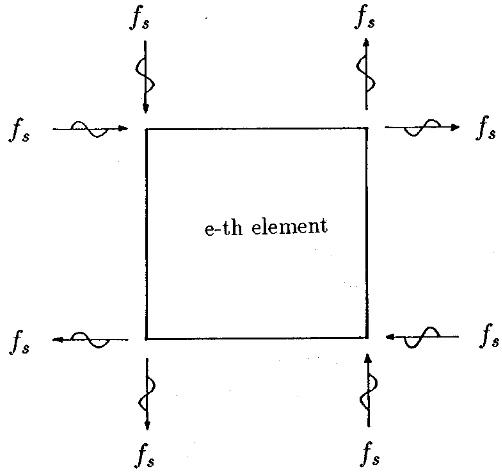

Fig. 7 (b) Equivalent nodal forces for reflected S-waves.

square element with an incident wave in the direction $e=(0, -1)$. Let a square element be centered at the origin with its side length $2h$ (Fig. 6). The crack is on the x-axis, and we set $\tau=(1, 0)$, $\theta=\pi/2$.

The shape function is defined as

$$[N_{ij}]=\begin{bmatrix} N_1 & 0 & N_2 & 0 & N_3 & 0 & N_4 & 0 \\ 0 & N_1 & 0 & N_2 & 0 & N_3 & 0 & N_4 \end{bmatrix} \qquad \cdots\cdots (21)$$

where

$$N_1=\frac{1}{4}(1+\xi_1)(1+\xi_2);\quad N_2=\frac{1}{4}(1-\xi_1)(1+\xi_2);$$

$$N_3=\frac{1}{4}(1-\xi_1)(1-\xi_2);\quad N_4=\frac{1}{4}(1+\xi_1)(1-\xi_2);$$

and $\xi_1=x/h$, $\xi_2=y/h$.

For the incident longitudinal waves, the matrix $[V^k_{ij}]$ has the form

$$[V^k_{jq}]=\begin{bmatrix} -2u_0(V_p^2-2V_s^2)\exp(i\omega_0 t) & 0 \\ 0 & -2u_0V_p^2\exp(i\omega_0 t) \end{bmatrix} \qquad \cdots\cdots (22)$$

Then, the equivalent nodal force vector due to the scattering P-waves is obtained as

$$\{P^*_i\}=\frac{1}{2}\rho u_0 V_p^2 \exp(i\omega_0 t)\begin{Bmatrix} 1-2\lambda \\ 1 \\ -(1-2\lambda) \\ 1 \\ -(1-2\lambda) \\ -1 \\ 1-2\lambda \\ -1 \end{Bmatrix} \qquad \cdots\cdots (23)$$

Similarly, for the incident transverse waves

$$[V^k_{jq}]=\begin{bmatrix} 0 & -2u_0V_s^2\exp(i\omega_0 t) \\ -2u_0V_s^2\exp(i\omega_0 t) & 0 \end{bmatrix} \qquad \cdots\cdots (24)$$

and the equivalent nodal force vector due to the scattering SV-wave is obtained as

$$\{P_i^*\}=\frac{1}{2}\rho u_0 V_s^2 \exp(i\omega_0 t)\begin{Bmatrix} 1 \\ 1 \\ 1 \\ -1 \\ -1 \\ -1 \\ -1 \\ 1 \end{Bmatrix} \qquad (25)$$

The nodal forces of the e-th element for the scattering of P-waves and SV-waves are illustrated in the Fig. 7. Firstly, let us consider the case of P-wave in Fig. 7(a). The total forces either in the x-direction or in the y-direction are all zero. The effect of the scattering waves is equivalent to two couples of tensile forces acting in the x- and y-directions, respectively. The conventional wave theory states that if a longitudinal wave is input vertically against a crack, we have not only the reflected longitudinal wave but also the reflected SV-wave. We can observe that such the tip effect is described as a tensile force acting in the x-direction in the presented model as shown in Fig. 7(a).

On the other hand, if a transverse wave is input, the equivalent force works as two couples of moment which balance each other. The reflection wave results in a change of the shape of the element.

(3) Numerical results

We show a numerical example for a specimen containing two cracks. The specimen has a rectangular shape with the size of 2.6×2.0 m^2 and the crack configuration is shown in Fig. 8. The numerical analysis is carried out for two cases : One is the case that the angle θ of the crack to the x-axis is 0°, and another is the case $\theta=45^\circ$. The lengths of the cracks are 0.7 m for $\theta=0^\circ$ and 0.707 m for $\theta=45^\circ$. The material constants are $V_p=1\,500$ m/s, $V_s=1\,000$ m/s and the mass density $\rho=1.2$ t/m^3.

The finite elements are all square with a side length of 0.1 m. The loads are applied in terms of the sinusoidal longitudinal and transverse displacement waves with an amplitude $u_0=1.0\times10^{-4}$ m and angular frequency $\omega=2\pi f$, $f=50$ Hz, $0\leq t\leq40$ ms on the top of the specimen as shown in Fig. 8.

For simulating the wave propagation in an infinite medium, the viscous dashpots[6),10)] are arranged on the four sides of the specimen. The central difference scheme is used for the time discretization of Eq. (17) with the increment of 0.008 ms.

Here, we also check the accuracy of the results calculated by the proposed method by comparing with

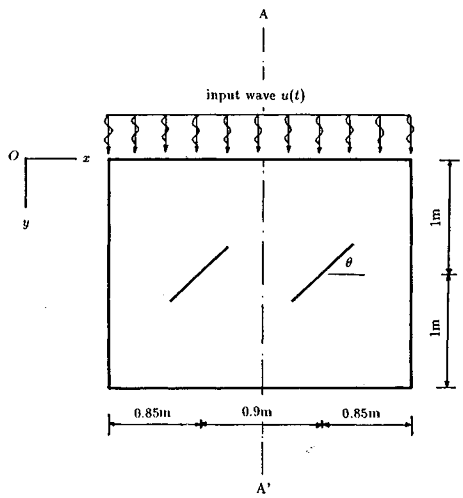

Fig. 8 Model involving two cracks.

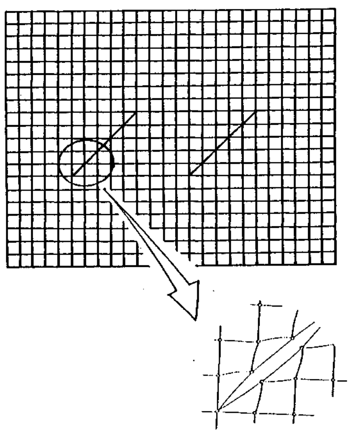

Fig. 9 Discontinuous model for conventional finite element analysis.

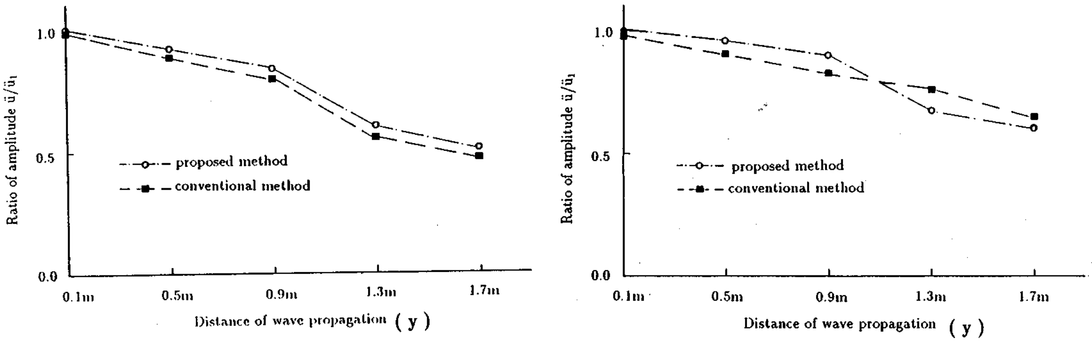

(a) $\theta=0°$ (b) $\theta=45°$

Fig. 10 Responses of P-wave.

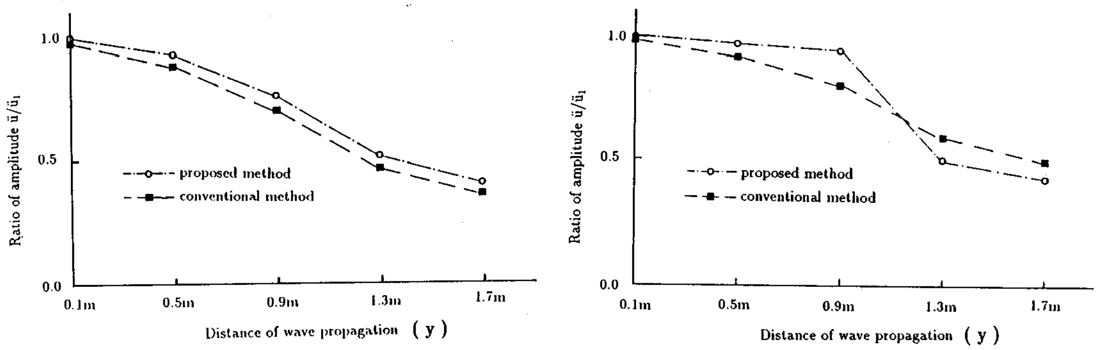

(a) $\theta=0°$ (b) $\theta=45°$

Fig. 11 Responses of S-wave.

those of a conventional method in which cracks are arranged explicitly in the finite element mesh[5] (**Fig. 9**). **Fig. 10** and **Fig. 11** show the amplitude responses where the circular symbols represent the results calculated by the proposed method and the rectangular symbols are the results calculated by the conventional method. The results plotted in the figures are the ones along the line A—A′ in **Fig. 8**. The normalizing acceleration $\ddot{u}_1$ is the value at position $y=0.1$ m. It is noted that the results obtained by the methods are agreed very well, particularly for P-wave. In **Fig. 11** (b), for S-wave, at the positions of $y=0.9$ m, 1.3 m, there is a somewhat difference between the results of both methods. This may be caused by the effect of multiple reflection of waves between the cracks. For the case of P-waves, such effect is very small.

5. CONCLUSION

The wave propagation in rock mass is very much affected by existing cracks. However, if the effect of each individual crack is to be taken into account, this problem becomes very complicated. No efficient method has ever been proposed to treat this problem. Some specific numerical methods such as the joint element can be applied merely for characterizing the behaviour of cracks. Those methods have several disadvantages in association with the mesh divisions if the number of cracks increases and their distributed configuration becomes complicated. In this paper, an approach to evaluate the effect of cracks in wave field is presented in which the effect of cracks is transformed into an equivalent nodal force. Its validity is checked by an example. The conclusions are as follows : The effect of cracks in the wave field can be evaluated as an equivalent nodal force in the numerical procedure. The effects of reflected P- and S-waves are evaluated as a couple of tensile force and two moments, respectively, and the total force in both cases is zero. The results of calculations show very good agreement between the proposed and conventional methods. The proposed method is very convenient since it is only necessary to calculate the equivalent nodal force.

For the practical application of the proposed method, some questions are still open. One is that how to describe the multiple reflection of waves between cracks if the distances of the cracks are small. As we indicated in the numerical example, the transverse waves may be more sensitive in this case. Although we here treat the plane problem for the isotropic linear elastic material only, it can be easily extended to the three dimensional problem with anisotropic material properties. Furthermore, since the cracks in rock mass are not always open, which may be filled with other materials, the proposed method can be modified to treat such problems.

ACKNOWLEDGEMENTS

The authors gratefully acknowledge to Dr. T. Kyoya and Mr. Ö. Aydan of Nagoya University, for their valuable discussions. The numerical analyses were performed at the Computation Center of Nagoya University.

REFERENCES

1) Achenbach, J. D., Gautesen, A. K. and McMaken, H. : Application of Elasto-Dynamic Ray Theory to Diffraction by Cracks, Modern Problems in Elastic Wave Propagation, John Wiley and Sons, pp. 219-237, 1977.
2) Aki, K. and Richards, P. G. : Quantitative Seismology Theory and Methods, Vol. 1, W. H. Freeman and Company, 1980.
3) Anderson, D. L., Minsier, B. and Cole, D. : The Effect of Oriented Cracks on Seismic Velocities, J. of Geophys. Res., Vol. 79, No. 26, pp. 4011-4015, 1974.
4) Burridge, R. and Knopoff, L. : Body Force Equivalents for Seismic Dislocations, Bulletin of Seismological Society of America, Vol. 54, pp. 1875-1888, 1964.
5) Han, S., Kyoya, T., Ichikawa, Y. and Kawamoto, T. : A Dynamic Analysis of Jointed Rock Mass, Proc. Int. Symp. Engng. in Complex Rock Formation, pp. 338-344, 1986.
6) Han, S., Kyoya, T., Ichikawa, Y. and Kawamoto, T. : A Study on the Dynamic Behaviors of Discontinuous Rock Mass with Damage Mechanics Theory, Proc. JSCE, Vol. 400/Ⅲ-3, pp. 65-74, 1988 (in Japanese).
7) Hanya, A., Lenartowicz, E. and Pajchel, J. : Seismic Wave Propagation in the Earth, PWN-Polish Scientific Publishers, 1985.
8) Jones, D. S. : On the Scattering Cross Section of an Obstacle, Phil. Mag., Vol. 46, pp. 957-962, 1985.
9) Kotoul, M. and Bilek, Z. : Waves of Fracture in Brittle Bodies, Engng. Fracture Mechanics, Vol. 27, No. 5, pp. 517-538, 1987.
10) Lysmer, J. and Kuhlemeyer, R. L. : Finite Dynamic Model for Infinite Media, EM 4, ASCE, pp. 859-877, 1969.
11) Mal, A. K. : Interaction of Elastic Waves with a Griffth Crack, Int. J. Engng. Sci., Vol. 8, pp. 763-776, 1970.
12) Piau, M. : Attenuation of a Plane Compressional Wave by a Random Distribution of Thin Circular Cracks, Int. J. Engng. Sci., Vol. 17, pp. 151-167, 1979.
13) Roy, A. : Diffraction of Elastic Waves by an Elliptic Crack, Int. J. Engng. Sci., Vol. 22, No. 6, pp. 729-739, 1984.
14) Zhang, C. H. and Achenbach, J. D. : Scattering by Multiple Cracks Configurations, Transaction of the ASME, Vol. 55, pp. 104-110, 1988.

(Received March 13 1989)